Optics EXPRESS

High-power low-noise 2-GHz femtosecond laser oscillator at 2.4 µm

AJANTA BARH,[1,*] B. ÖZGÜR ALAYDIN,[1,2] JONAS HEIDRICH,[1] MARCO GAULKE,[1] MATTHIAS GOLLING,[1] CHRISTOPHER R. PHILLIPS,[1] AND URSULA KELLER[1]

[1] *Department of Physics, Institute of Quantum Electronics, ETH Zurich, Auguste-Piccard-Hof 1, 8093 Zurich, Switzerland*
[2] *Current address: Department of Physics, Sivas Cumhuriyet University, 58140 Merkez/Sivas, Turkey*
[*] *ajbarh@phys.ethz.ch*

Abstract: Femtosecond lasers with high repetition rates are attractive for spectroscopic applications with high sampling rates, high power per comb line, and resolvable lines. However, at long wavelengths beyond 2 µm, current laser sources are either limited to low output power or repetition rates below 1 GHz. Here we present an ultrafast laser oscillator operating with high output power at multi-GHz repetition rate. The laser produces transform-limited 155-fs pulses at a repetition rate of 2 GHz, and an average power of 0.8 W, reaching up to 0.7 mW per comb line at the center wavelength of 2.38 µm. We have achieved this milestone via a Cr^{2+}-doped ZnS solid-state laser modelocked with an InGaSb/GaSb SESAM. The laser is stable over several hours of operation. The integrated relative intensity noise is 0.15% rms for [10 Hz, 100 MHz], and the laser becomes shot noise limited (-160 dBc/Hz) at frequencies above 10 MHz. Our timing jitter measurements reveal contributions from pump laser noise and relaxation oscillations, with a timing jitter of 100 fs integrated over [3 kHz, 100 MHz]. These results open up a path towards fast and sensitive spectroscopy directly above 2 µm.

1. Introduction

Optical frequency combs (OFC) with gigahertz line spacing are powerful tools for applications such as high-precision frequency metrology [1], rapid spectroscopy with resolved comb lines [2,3], terabit communication [4], and low-damage bio-tissue analysis [5]. Though most of the current technologies operate at visible and near-infrared wavelengths, there is a surge in mid-infrared and short-wave infrared applications [6]. This trend motivates the development of GHz sources with high power beyond 2 µm.

Many high-power mid-infrared OFCs are based on frequency down-conversion of near-infrared lasers [7,8]. While they can provide Watt-level average power, they utilize a complex architecture and typically operate at lower repetition rates. On the other hand, a frequency conversion based microresonator comb has been recently demonstrated at 10 GHz, but their waveguiding geometry limits the power to the 100-µW level [9]. State-of-the-art quantum cascade lasers (QCL) emit directly in the mid-infrared [10] and can provide 10's of mW average power, however they work with larger comb spacing, typically well above 10 GHz [3]. Modelocked semiconductor vertical external cavity surface emitting lasers (VECSEL) at 2 µm are in their infancy and limited to mW power level [11]. Finally, ion-doped fiber and solid-state ultrafast oscillators operating above 2 µm [12] are currently limited to either megahertz repetition rates for Watt-level operation [13–16], or can deliver pulses above GHz repetition rates but with a limited average power (10's of mW) [17,18]. Recently a master oscillator power amplifier based solid-state laser system above 2-µm is proposed with 6 W average power at 0.9 GHz repetition rate [19]. However, there still exists a trade-off between the comb line spacing and power scaling of the state-of-the-art modelocked oscillators operating in the important 2-µm range.

#446986 https://doi.org/10.1364/OE.446986
Journal © 2022 Received 3 Nov 2021; revised 20 Dec 2021; accepted 21 Jan 2022; published 2 Feb 2022

Optics EXPRESS

In this work, we overcome this trade-off and demonstrate a compact and stable fundamentally modelocked ultrafast solid-state laser operating directly above 2 µm. The oscillator delivers 155-fs pulses at record-high 2-GHz repetition rate (> 2× higher than the reported result in [19]) with an average power of 0.8 W. The power per comb line reaches up to 0.7 mW at the center wavelength of 2.38 µm. We have achieved this by using a commercial Cr^{2+}-doped ZnS gain medium and a high-performance InGaSb/GaSb quantum well semiconductor saturable absorber mirror (SESAM) which stabilizes soliton modelocking even at this multi-GHz operation [20]. Note that, in comparison to any saturable absorber modelocked Cr-laser, our result reports 8× increase in average power and >2× increase in repetition rate [21].

Optically pumped Cr^{2+}-doped ZnS/ZnSe solid-state lasers have shown wide wavelength tunability covering the entire 2–3 µm range [22,23] with few-cycle pulse generation [24,25] and high power operation [13–15,19]. The state-of-the-art performances are achieved using Kerr-lens modelocking (KLM), however mostly at lower repetition rates (100-MHz range). While KLM [26] is ideal for few-cycle pulse generation, SESAMs [27] are advantageous for low-noise, robust, and self-starting modelocking. The lack of low-loss and fast SESAMs at these long wavelengths has hindered the lasing performance. Recently, we have successfully developed a high-quality 2.4-µm SESAM and demonstrated Watt-level average power at a repetition rate of 250 MHz [13]. The antiresonant SESAM design [27] consists of 3× type-I InGaSb/GaSb quantum wells on top of a 24-pair of AlAsSb/GaSb distributed Bragg reflector, giving a total epitaxial layer thickness of only 8.35 µm on the GaSb substrate. Saturation measurement [28] of the SESAM at 2.4 µm reveals favorable parameters: low saturation fluence (10.5 µJ/cm^2), sufficient modulation depth (1.6%), and low nonsaturable losses (0.8%). Furthermore, the SESAM has a fast absorber recovery time of <2 ps. These are the key SESAM parameters enabling high-power multi-GHz operation of our laser, as reported herein.

2. Laser cavity design

The six-element laser cavity is shown in Fig. 1(a), where a polycrystalline Cr:ZnS gain medium with doping concentration of 9×10^{18}/cm^3 (IPG Photonics) is placed between two concave mirrors of a standard Z-shape cavity. The crystal is 3.8 mm long and Brewster cut. It is mounted on a water-cooled thermo-electric controlled copper mount and temperature stabilized to 16°C. A 1550-nm Er-fiber laser (NKT Photonics) providing up to 10 W of cw output power is used for pumping. In order to achieve gigahertz repetition rates, we use two concave cavity turning mirrors (M1 and M2) of 20 mm radii. Both the mirrors are ion beam sputtering (IBS) coated for broadband high reflection over 2.1–3.0 µm and transmit the pump wavelength. The flat output coupler (OC) is IBS coated for ~ 3% average transmission over 2.2–2.6 µm. The SESAM, working as a flat end mirror, is mounted on a copper block without any active thermal stabilization. All dielectric mirror coatings provide nearly flat group delay dispersion (GDD).

Soliton formation is the main pulse shaping mechanism in our case. In order to obtain a suitable round-trip GDD for fundamental soliton formation, we inserted an uncoated 4-mm-long YAG window (which has negative GDD) at Brewster's angle inside the cavity. The estimated round-trip GDD of the cavity elements and the ideal GDD required for soliton condition is plotted in Fig. 1(b). The measured linear reflectivity of the SESAM shows >99.5% over a bandwidth of 110 nm. The astigmatism introduced by the gain element and YAG window is minimized by choosing incident angles on the curved mirrors of ~ 10°. The laser is mounted on an optical breadboard and operated in a standard laboratory environment. The compact cavity is only 7.4 cm long, giving a repetition rate of ~ 2 GHz. A challenge for such short cavity is its reduced design flexibility. Additionally, the low intracavity pulse energy reduces the effective cavity nonlinearity, making the soliton formation more challenging. In our case, the pump and laser spot sizes (radii) at the input facet of the gain medium are 35 µm and 46 µm, respectively. Additionally, it requires a tighter focus to saturate the SESAM such that the cw-modelocking threshold is reached at the

Optics EXPRESS

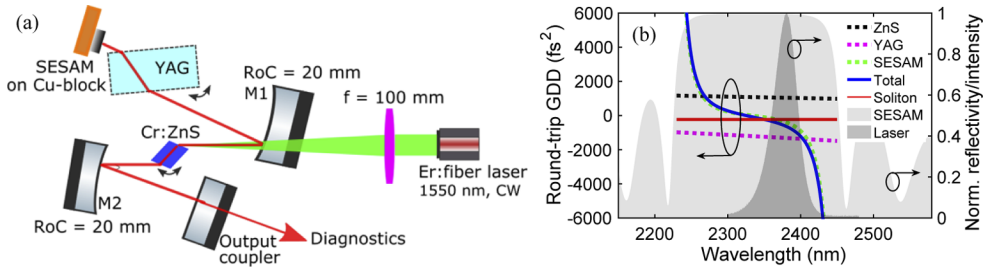

Fig. 1. (a) Schematic of the compact 2-GHz Cr:ZnS laser cavity. The gain element and YAG crystal are mounted on translation-rotation stages. (b) The estimated round-trip GDD of the cavity elements and the measured reflectivity of the SESAM (light grey solid). GDD of ZnS (black dashed), YAG (pink dashed), SESAM (green dashed), and total GDD (blue solid) is plotted. The red solid is the GDD needed to satisfy the soliton condition for 150 fs pulses at 0.8 W of average output power. The measured laser spectrum at highest modelocked power (dark grey solid) is aligned closely to the expected position.

available power. The best modelocking performance is achieved while operating the SESAM in a strongly saturated regime with intracavity fluence close to its reflectivity roll-over [28]. With the estimated laser spot size (radius) on SESAM of ~155 µm, the average fluence (i.e., half the peak fluence for a Gaussian beam) is 17 µJ/cm^2 at the highest modelocked output power. The corresponding measured laser spectrum is also plotted in Fig. 1(b) to obtain a direct comparison between the estimated cavity parameters and the resulting soliton spectrum.

3. Modelocking performance

With SESAM in place, self-starting soliton modelocking [20] is established over a wide range of laser output power (Fig. 2). We observe cw operation at low pump power and then with increasing pump power the laser transitions to a Q-switched modelocking regime [29]. At input pump power above 2.2 W a stable cw-modelocking is established for output average power of 400–800 mW. Close to transform limited pulse duration is achieved over this entire range (red and grey in Fig. 2), with shortest pulse duration of 155 fs at 800 mW. At this power level the estimated optical-to-optical efficiency with respect to absorbed pump power is ~ 26%, comparable to standard KLM oscillators [23].

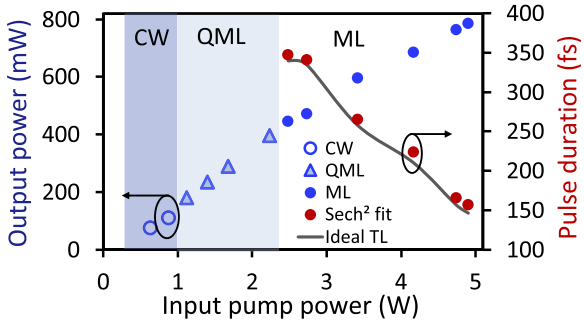

Fig. 2. Modelocking performance. Measured output average power (cw: blue open circle, Q-switched modelocking (QML): blue triangle, Modelocking (ML): blue solid circle) and pulse duration (red, ideal transform limited (TL) fit in grey) for different input pump power.

The measured intensity autocorrelator trace is shown in Fig. 3(a). Inset shows the measured optical spectrum with a full-width at half-maximum bandwidth (FWHM) of 41 nm centered

Optics EXPRESS

at 2.38 µm. The corresponding time-bandwidth product (TBP) is 0.335 (1.06 × the transform limit for an ideal sech^2 pulse). The decrease in pulse duration with increasing pump power is a strong indication of a soliton modelocking mechanism for the pulse formation. Further increase in pump power resulted in damaging the coating of one intracavity mirror. Because of the lack of high-speed photodetectors at 2.4 µm, a direct measurement of the pulse repetition rate was not possible. Instead, we have used an external second harmonic generation (SHG) based measurement using a periodically poled lithium niobate crystal, where the SHG of the laser output is detected using a fast (18 GHz) InGaAs detector connected to a 26-GHz microwave spectrum analyzer. A clean radio frequency spectrum is recorded (Fig. 3(b)) indicating fundamental modelocking at repetition rate of 2.04 GHz. The pulse energy becomes 0.4 nJ, corresponding to a peak power of 2.5 kW. The estimated power per comb line is > 0.1 mW over a 70 nm bandwidth and reaches up to 0.7 mW at center wavelength of 2.38 µm. To date this has been the highest repetition rate achieved at this 2-µm range for any type of modelocked femtosecond laser with high output power. Even at this high-power level we did not observe any SESAM damage and the power stability of the laser is recorded over 3 hours (Fig. 3(c)) using a thermal power meter (Thorlabs S425C). The inset shows the measured beam profile using a microbolometer camera. The beam quality is measured (Fig. 3(d)) using a scanning slit profiler (Beam'R2) featuring an extended InGaAs detector and a scanning stage. An excellent beam quality with M^2 <1.15 is measured for both the axes.

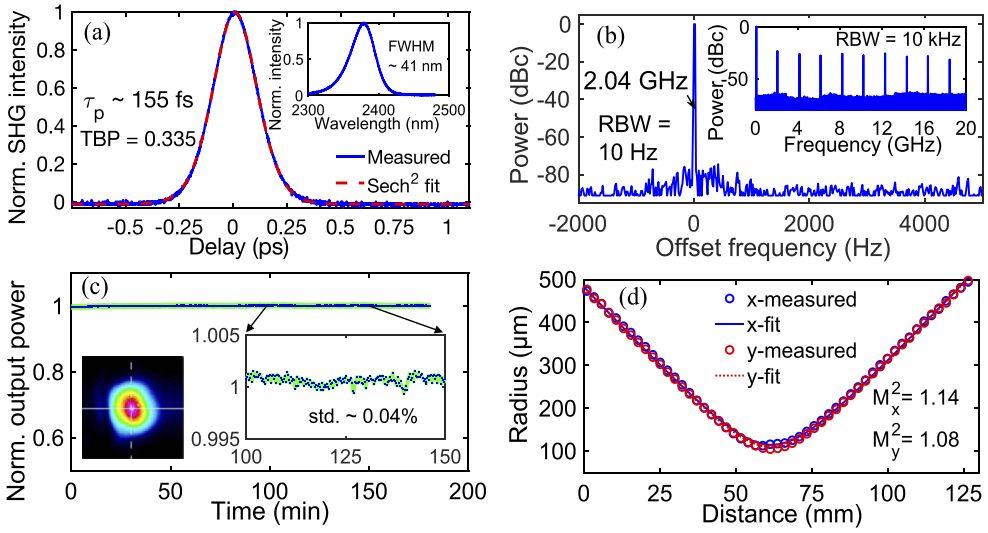

Fig. 3. Laser performance at highest average output power of 0.8 W. (a) Autocorrelation trace with sech^2 fit. The inset shows the measured optical spectrum. (b) Radio frequency (RF) trace centered at 2.04 GHz and measured with a resolution bandwidth (RBW) of 10 Hz and a span of 7 kHz. The inset shows the RF trace over a wider span of 20 GHz measured with a RBW of 10 kHz. (c) Output power stability over 3 hours. The standard deviation of power fluctuation over the indicated time window is ~0.04%. The inset shows the measured beam profile. (d) Measured M^2 of the laser beam.

4. Noise characterization

Next, we have measured both the relative intensity noise (RIN) and timing jitter to analyze the laser noise properties on shorter timescales. Our measurements show that these noise properties are dominated by the relaxation oscillations of the Cr:ZnS laser, the RIN of the Er-fiber pump, and shot noise.

Optics EXPRESS

The RIN is measured directly at the lasing wavelength at baseband by using a biased extended InGaAs photodiode (17 ns rise time) followed by an external amplifier and a signal source analyzer (SSA). To optimize the sensitivity of the measurement, two different electronic amplifier configurations are used to cover the entire bandwidth of our measurement, i.e., 10 Hz – 100 MHz. One is optimized for low frequencies (DC – 500 kHz) and other for high frequencies (20 kHz – 1 GHz). The two noise spectra are then stitched together at around 330 kHz to represent the entire RIN spectrum of the laser. We measure the noise at two different power levels (600 and 700 mW, Fig. 4(a)). To identify different noise sources, we have further measured (1) the contribution of the detection setup by blocking the light beam entering the photodetector (light blue and orange in Fig. 4(a)) and (2) the noise of the pump (Er-fiber laser) measured directly by using a highly linear InGaAs photodiode (DC – 22 GHz), green in Fig. 4(a). A current of 3.5 A is used for this pump noise measurement, which corresponds to a modelocked laser power of about 700 mW. The dominant noise source between 5 kHz and 2 MHz is coming from the pump itself, which could be reduced by, for example, using a laser diode for pumping [24]. Another noise peak occurs around 4 MHz range, which is estimated to be related to the relaxation oscillations (RO) of the Cr:ZnS oscillator. This feature becomes smaller and also shifts towards higher frequency at higher power. For the lower frequencies below 4-5 kHz, the RIN curve for the 1550-nm pump is dominated by the measurement electronics. Thus, in this low-frequency range the laser RIN is not necessarily due to pump RIN. For example, we have found that a constant flow of N_2 on the cavity significantly reduces laser RIN below 1 kHz. So, factors other than the pump have a strong influence at these frequencies. The integrated RMS noise of this free-running laser is 0.15% for integration from 10 Hz – 100 MHz. Importantly, beyond the RO peak the RIN measurement is fundamentally shot noise limited at -160 dBc/Hz.

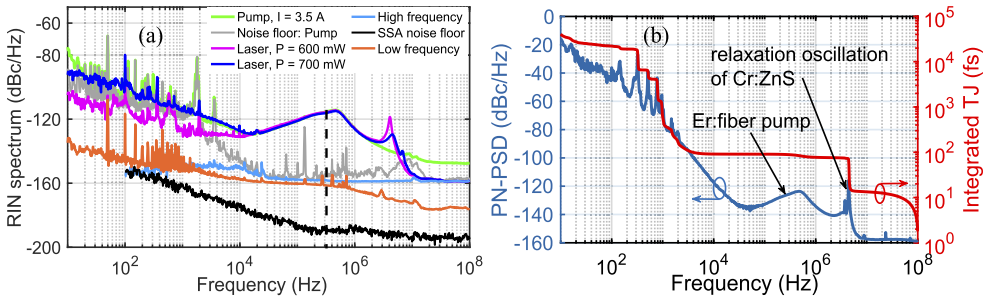

Fig. 4. (a) Relative intensity noise spectrum of the free-running 2-GHz Cr:ZnS oscillator at output power (P) of 600 mW (pink) and 700 mW (blue). Vertical dashed line shows the stitching frequency of the two measurements. Noise floor for the low-frequency (DC-500 kHz, orange) and high-frequency (20 kHz – 1 GHz, light blue) measurements. Green: RIN of the Er-fiber pump. Light grey: noise floor of pump noise measurement. Black: SSA noise floor. (b) Phase noise power spectral density (PN-PSD, blue) and integrated timing jitter (TJ, red) of SHG signal of the laser at 700 mW output power.

For the timing jitter measurement, we have used the SHG signal of the laser and measured the phase noise (PN) of the 1st harmonic of the repetition rate at 2 GHz with the highly linear InGaAs photodiode connected to two band-pass filters, a pre-amplifier (0.1–18 GHz) and then SSA. The power spectral density is shown in Fig. 4(b) (blue). The integrated PN (red, Fig. 4(b)) indicates a timing jitter of 100 fs for integration from 3 kHz – 100 MHz. The noise at lower frequencies likely originates from mechanical noise sources which were not optimized in this laser setup. For frequencies above the RO frequency of the laser, the integrated timing jitter is below 10 fs. Furthermore, we have estimated the effect of the phase noise on the comb optical linewidth using the beta-separation line approximation [30]. A significant contribution comes

Optics EXPRESS

from the pump and the laser RIN at high frequencies. However, one can achieve 10-MHz range linewidths for measurement time below 1 µs using such a free-running 2-GHz laser.

5. Conclusion

In conclusion, to the best of our knowledge, we demonstrate the highest repetition rate modelocked laser operating above 2 µm and generating femtosecond pulses at high power. This breakthrough result is achieved in a Cr:ZnS solid-state laser passively modelocked with a home-grown high-performance InGaSb/GaSb quantum well SESAM. The laser delivers 155 fs pulses at 2 GHz repetition rate with 0.8 W of average power, corresponding to a peak power of 2.5 kW directly from the oscillator. Further power scaling can be done by considering a higher output coupling rate. Additional dispersion management, for example a SESAM with flatter dispersion profile, should enable even shorter pulses. The laser shows excellent power stability over 3 hours with good beam quality. The short-term noise is primarily dominated by relaxation oscillations of the Er-fiber pump and the Cr:ZnS laser itself. However, even in the free-running condition an integrated RMS noise below 0.15% is achieved with timing jitter of 100 fs over 3 kHz – 100 MHz. Moreover, above 10 MHz the measurement is shot noise limited at -160 dBc/Hz. Since high-speed measurements such as dual-comb spectroscopy would produce signals at such frequencies, this low-noise is of great interest for high-sensitivity spectroscopic applications. Our result paves the way towards a new class of multi-GHz high-power low-noise femtosecond oscillators operating directly in the important 2–3 µm range, suitable for ultrafast spectroscopy and efficient nonlinear frequency conversion.

Funding. European Research Council (ERC advanced grant 787097 ONE-MIX).

Acknowledgments. We thank FIRST cleanroom facility of ETH Zurich, and Dr. V. Wittwer of U. of. Neuchatel for the coating on output coupler. A. B. thanks M. Baer of ETH Zurich for useful discussion on mechanical design, and S. Camenzind of ETH Zurich for helping with the noise measurement.

Disclosures. The authors declare no conflicts of interest.

Data availability. Data underlying the results presented in this paper are not publicly available at this time but may be obtained from the authors upon reasonable request.

References

1. T. Udem, R. Holzwarth, and T. W. Hänsch, "Optical frequency metrology," Nature **416**(6877), 233–237 (2002).
2. S. A. Diddams, L. Hollberg, and V. Mbele, "Molecular fingerprinting with the resolved modes of a femtosecond laser frequency comb," Nature **445**(7128), 627–630 (2007).
3. G. Villares, A. Hugi, S. Blaser, and J. Faist, "Dual-comb spectroscopy based on quantum-cascade-laser frequency combs," Nat. Commun. **5**(1), 5192 (2014).
4. H. Hu, F. Da Ros, M. Pu, F. Ye, K. Ingerslev, E. Porto da Silva, M. Nooruzzaman, Y. Amma, Y. Sasaki, T. Mizuno, Y. Miyamoto, L. Ottaviano, E. Semenova, P. Guan, D. Zibar, M. Galili, K. Yvind, T. Morioka, and L. K. Oxenløwe, "Single-source chip-based frequency comb enabling extreme parallel data transmission," Nat. Photonics **12**(8), 469–473 (2018).
5. S.-W. Chu, T.-M. Liu, C.-K. Sun, C.-Y. Lin, and H.-J. Tsai, "Real-time second-harmonic-generation microscopy based on a 2-GHz repetition rate Ti:sapphire laser," Opt. Express **11**(8), 933–938 (2003).
6. A. Schliesser, N. Picqué, and T. W. Hänsch, "Mid-infrared frequency combs," Nat. Photonics **6**(7), 440–449 (2012).
7. C. Gaida, M. Gebhardt, T. Heuermann, F. Stutzki, C. Jauregui, J. Antonio-Lopez, A. Schülzgen, R. Amezcua-Correa, A. Tünnermann, I. Pupeza, and J. Limpert, "Watt-scale super-octave mid-infrared intrapulse difference frequency generation," Light: Sci. Appl. **7**(1), 94 (2018).
8. S. Parsa, S. C. Kumar, B. Nandy, and M. Ebrahim-Zadeh, "Yb-fiber-pumped, high-beam-quality, idler-resonant mid-infrared picosecond optical parametric oscillator," Opt. Express **27**(18), 25436–25444 (2019).
9. A. S. Kowligy, D. R. Carlson, D. D. Hickstein, H. Timmers, A. J. Lind, P. G. Schunemann, S. B. Papp, and S. A. Diddams, "Mid-infrared frequency combs at 10 GHz," Opt. Lett. **45**(13), 3677–3680 (2020).
10. A. Hugi, G. Villares, S. Blaser, H. C. Liu, and J. Faist, "Mid-infrared frequency comb based on a quantum cascade laser," Nature **492**(7428), 229–233 (2012).
11. A. Härkönen, C. Grebing, J. Paajaste, R. Koskinen, J.- Alanko, S. Suomalainen, G. Steinmeyer, and M. Guina, "Modelocked GaSb disk laser producing 384 fs pulses at 2 µm wavelength," Electron. Lett. **47**(7), 454–456 (2011).
12. J. Ma, Z. Qin, G. Xie, L. Qian, and D. Tang, "Review of mid-infrared mode-locked laser sources in the 2.0 µm–3.5 µm spectral region," Appl. Phys. Rev. **6**(2), 021317 (2019).

Optics EXPRESS

13. A. Barh, J. Heidrich, B. O. Alaydin, M. Gaulke, M. Golling, C. R. Phillips, and U. Keller, "Watt-level and sub-100-fs self-starting mode-locked 2.4-µm Cr:ZnS oscillator enabled by GaSb-SESAMs," Opt. Express **29**(4), 5934–5946 (2021).
14. E. Sorokin, N. Tolstik, and I. T. Sorokina, "1 Watt femtosecond mid-IR Cr:ZnS laser," Proc. SPIE **8599**, 859916 (2013).
15. S. Vasilyev, I. Moskalev, M. Mirov, S. Mirov, and V. Gapontsev, "Multi-Watt mid-IR femtosecond polycrystalline Crˆ2+:ZnS and Crˆ2+:ZnSe laser amplifiers with the spectrum spanning 20–26 µm," Opt. Express **24**(2), 1616–1623 (2016).
16. J. Huang, M. Pang, X. Jiang, F. Köttig, D. Schade, W. He, M. Butryn, and P. S. J. Russell, "Sub-two-cycle octave-spanning mid-infrared fiber laser," Optica **7**(6), 574–579 (2020).
17. J. Zeng, A. E. Akosman, and M. Y. Sander, "Scaling the repetition rate of thulium-doped ultrafast soliton fiber lasers to the GHz regime," Opt. Express **26**(19), 24687–24694 (2018).
18. Y. Wang, J. Li, K. Mo, Y. Wang, F. Liu, and Y. Liu, "14.5 GHz passive harmonic mode-locking in a dispersion compensated Tm-doped fiber laser," Sci. Rep. **7**(1), 7779 (2017).
19. V. Smolski, S. Vasilyev, I. Moskalev, M. Mirov, Q. Ru, A. Muraviev, P. Schunemann, S. Mirov, V. Gapontsev, and K. Vodopyanov, "Half-Watt average power femtosecond source spanning 3–8 µm based on subharmonic generation in GaAs," Appl. Phys. B **124**(6), 101 (2018).
20. F. X. Kartner, I. D. Jung, and U. Keller, "Soliton mode-locking with saturable absorbers," IEEE J. Sel. Top. Quantum Electron. **2**(3), 540–556 (1996).
21. N. Tolstik, E. Sorokin, and I. T. Sorokina, "Gigahertz femtosecond Cr:ZnS laser," in *Advanced Solid State Lasers* (OSA, 2014), paper AM3A.
22. S. B. Mirov, I. S. Moskalev, S. Vasilyev, V. Smolski, V. V. Fedorov, D. Martyshkin, J. Peppers, M. Mirov, A. Dergachev, and V. Gapontsev, "Frontiers of Mid-IR Lasers Based on Transition Metal Doped Chalcogenides," IEEE J. Sel. Top. Quantum Electron. **24**(5), 1–29 (2018).
23. I. T. Sorokina and E. Sorokin, "Femtosecond Cr^{2+}-Based Lasers," IEEE J. Sel. Top. Quantum Electron. **21**(1), 273–291 (2015).
24. N. Nagl, S. Gröbmeyer, V. Pervak, F. Krausz, O. Pronin, and K. F. Mak, "Directly diode-pumped, Kerr-lens mode-locked, few-cycle Cr:ZnSe oscillator," Opt. Express **27**(17), 24445–24454 (2019).
25. S. Vasilyev, I. Moskalev, V. Smolski, J. Peppers, M. Mirov, V. Fedorov, D. Martyshkin, S. Mirov, and V. Gapontsev, "Octave-spanning Cr:ZnS femtosecond laser with intrinsic nonlinear interferometry," Optica **6**(2), 126–127 (2019).
26. D. E. Spence, P. N. Kean, and W. Sibbett, "60-fsec pulse generation from a self-mode-locked Ti:sapphire laser," Opt. Lett. **16**(1), 42–44 (1991).
27. U. Keller, K. J. Weingarten, F. X. Kartner, D. Kopf, B. Braun, I. D. Jung, R. Fluck, C. Honninger, N. Matuschek, and J. A. der Au, "Semiconductor saturable absorber mirrors (SESAM's) for femtosecond to nanosecond pulse generation in solid-state lasers," IEEE J. Sel. Top. Quantum Electron. **2**(3), 435–453 (1996).
28. J. Heidrich, M. Gaulke, B. O. Alaydin, M. Golling, A. Barh, and U. Keller, "Full optical SESAM characterization methods in the 1.9 to 3-µm wavelength regime," Opt. Express **29**(5), 6647–6656 (2021).
29. C. Hönninger, R. Paschotta, F. Morier-Genoud, M. Moser, and U. Keller, "Q-switching stability limits of continuous-wave passive mode locking," J. Opt. Soc. Am. B **16**(1), 46–56 (1999).
30. G. D. Domenico, S. Schilt, and P. Thomann, "Simple approach to the relation between laser frequency noise and laser line shape," Appl. Opt. **49**(25), 4801–4807 (2010).